Micromorphological Characterization of Zinc/Silver Particle Composite Coatings

ALIA MÉNDEZ,[1] YOLANDA REYES,[2] GABRIEL TREJO,[2] KRZYSZTOF STĘPIEŃ,[3] AND ŞTEFAN ŢĂLU[4]*
[1]*Department of Applied Bioinorganic, Centro De Química-ICUAP Benemérita Universidad Autónoma De Puebla, Ciudad Universitaria Puebla, Puebla 72530, México*
[2]*Department of Surface Coatings and Composite Materials, Parque Tecnológico Sanfandila, Centro De Investigación Y Desarrollo Tecnológico En Electroquímica (CIDETEQ), Pedro Escobedo, Querétaro, a. P. 064. C .P. 76703, Querétaro, México*
[3]*Faculty of Mechatronics and Mechanical Engineering, Department of Manufacturing Engineering and Metrology, Kielce University of Technology, Aleja 1000-Lecia Państwa Polskiego 7,*
Kielce 25-314, Poland
[4]*Faculty of Mechanical Engineering, Department of AET, Discipline of Descriptive Geometry and Engineering Graphics, Technical University of Cluj-Napoca, 103-105 B-Dul Muncii St., Cluj-Napoca, Cluj 400641, Romania*

KEY WORDS surfaces; zinc compounds; atomic force microscopy; nanomaterials; nanostructures; biomaterials

ABSTRACT The aim of this study was to evaluate the three-dimensional (3D) surface micromorphology of zinc/silver particles (Zn/AgPs) composite coatings with antibacterial activity prepared using an electrodeposition technique. These 3D nanostructures were investigated over square areas of 5 μm × 5 μm by atomic force microscopy (AFM), fractal, and wavelet analysis. The fractal analysis of 3D surface roughness revealed that (Zn/AgPs) composite coatings have fractal geometry. Triangulation method, based on the linear interpolation type, applied for AFM data was employed in order to characterise the surfaces topographically (in amplitude, spatial distribution and pattern of surface characteristics). The surface fractal dimension D_f, as well as height values distribution have been determined for the 3D nanostructure surfaces. *Microsc. Res. Tech. 78:1082–1089, 2015.*

INTRODUCTION

Zinc coatings provide the most effective and economical way to protect substrates to corrosion. Their dense and adherent corrosion byproducts, leads a rate of corrosion considerably lower than the protected substrate (Zhang, 1996).

On the other hand, it has been known for long time that metals such as silver and copper exhibit antimicrobial properties. For instance, silver-based compounds used as wound dressings and biocide in hospitals and other health care facilities have been used as bactericidal agent since the 19th century. Currently, an increasingly important field of research in inorganic antimicrobial material development is the use of silver nanoparticles (AgNPS) to enhance thermal resistance, stability and persistence of the antibacterial effects (Korai, 1999).

The combination of the unique physical properties of Zn coatings with the antimicrobial properties of AgNPs, open the possibility to make new inorganic antimicrobial material. In this regarding, it was previously reported (Grier, 1993) a zinc/silver particles (Zn/AgPs) composite presenting bactericidal activity, and self-hygienic capacity. The Ag nanoparticles were occludes in the coatings by means of electrochemical technique. To quantitatively describe the influence of AgPs concentration on the surface structure of Zn/AgPs composite and consequently its antimicrobial properties, a fractal analysis approaching was performed to different Ag particles content.

It is known that the most engineering surfaces possess a random surface texture: isotropic (Gaussian or non-Gaussian) or anisotropic, that is in correlation with the manufactured method (Kulesza and Bramowicz, 2014; Ţălu, 1998).

On the other hand, surface topography is an important characteristic in engineering surface design based on the precision and functional performance requirements (Lombardo et al., 2010; Stach et al., 2015; Ţălu, 2013). Topography descriptors can help in the assessment of the functional performance of different surface microtopographies; also, they can provide support to the development of virtual microtopography models specialized in the replication of specific aspects of a surface morphology (Senin and Groppetti, 2005).

Surface topography can be characterized using many statistical parameters depicting various aspects of the surface layer, roughness, waviness, and the form (Berezina et al., 2015).

To overcome the limits of the Euclidean approach, fractal geometry, has been used for quantifying the irregular complex structures and patterns across many spatial or temporal scales, relevant to

Correspondence to: Assoc. Prof. Ştefan Ţălu, Ph.D., Eng., Technical University of Cluj-Napoca, Faculty of Mechanical Engineering, Department of AET, Discipline of Descriptive Geometry and Engineering Graphics, 103-105 B-dul Muncii St., Cluj-Napoca 400641, Cluj, Romania. E-mail: stefan_ta@yahoo.com

REVIEW EDITOR: Prof. Alberto Diaspro

Received 3 August 2015; accepted in revised form 27 September 2015

DOI 10.1002/jemt.22588
Published online 24 October 2015 in Wiley Online Library (wileyonlinelibrary.com).

applications in biomedical imaging research, and medicine (Moldovan et al., 2015; Ţălu, 2012a,b; Ţălu et al., 2014a,b). Fractal geometry and scaling concepts can concisely as well as more effectively describe the 3D surfaces (Dallaeva et al., 2014; Elenkova et al., 2015; Ţălu et al., 2014c; Ţălu et al., 2015a).

A fractal 3D surface exhibits topographical features that are independent of the measurement scale and is characterised by a spatial scale-invariance (statistical self-similarity, which takes place only in the restricted range of the spatial scales) (Ţălu and Stach, 2014f; Ţălu et al., 2014d,e; 2015b,c,d).

It is known for a mass fractal (object), its mass M increases with its size (equivalent radius r) according to the relation (Pabst and Gregorova, 2007):

$$M \propto r^{\mathrm{Dm}} \tag{1}$$

where D_m is the mass fractal dimension ($0 \leq D_m \leq 3$). On the other hand, a surface fractal (object) has a surface area S increasing with its size (equivalent radius) proportional to r^{Df} (Pabst and Gregorova, 2007):

$$S \propto r^{\mathrm{Df}} \tag{2}$$

where D_f is the surface fractal dimension (a fractional value within the range $2 \leq D_f \leq 3$) to globally estimate the 3D fractal surface complexity (Dallaeva et al., 2014; Ţălu et al., 2014d, 2015b). For an Euclidian object (non-fractal with a smooth surface), $D_m = 3$, and $D_f = 2$; for mass fractal objects $D_m = D_f$, and for surface fractal objects $D_m = 3$, and $2 < D_f < 3$ (Pabst and Gregorova, 2007).

Several studies have reported morphological and electrochemical characterization of electrodeposited Zn–Ag nanoparticle composite coatings (Ahearn et al., 1995; Punith and Srivastava, 2013; Reyes-Vidal et al., 2015).

The purpose of this study was to investigate the 3D surface micromorphology of (Zn/AgPs) composite coatings with antibacterial activity prepared using an electrolytic bath with suspended Ag nanoparticles.

MATERIALS AND METHODS

Analysis of the Stability of Silver Particles in Suspension

A common method for producing an evenly occlusion of inert particles during the electrodeposition process of a metal, is by using a stable suspension of that inert particles as a part of the electrolytic bath. Stable suspensions are formed when soluble compounds are adsorbed onto the inert surface particle (Chen et al., 2003; Nguyen and Schulze, 2004). Surfactants or dispersants are commonly used to surface modification due to its space structure and hydrophilic functional groups, can enhance the electrostatic repulsion and steric hindrance between nanoparticles.

The following procedure was used to analyze the influence of the dispersant (surfactant) cetyltrymethylamonium bromide (CTAB) (98%, Spectrum lab, USA) on the stability of the silver particles in an electrolytic bath. First, 0.063 mg of AgNPs (99.9%, 50–60 nm, SkySpring Nanomaterials) was weighed and added to 25 mL of a base solution, S_0, (electrolytic bath) containing the following: 81.0 g L^{-1} $ZnCl_2$ + 208.80 g L^{-1} KCl + 25 g L^{-1} H_3BO_3 + 0.75 g L^{-1} sodium benzoate + 0.2 g L^{-1} benzylideneacetone + 1.5 g L^{-1} PEG + 2.8 g L^{-1} triethanolamine, at pH = 5.0. Next, the dispersant CTAB of the desired concentration (mM), was added to the solution to evaluate the long-term dispersion stability. Several concentrations of CTAB in the electrolytic bath were tested. The aqueous suspension of AgPs was placed into cylindrical glass vial and set in the Turbiscan Lab analyzer (Formulation, L'Unión, France). The transmission and back-scattered light sensors of this optical analyzer scanned the entire height (53 mm) of the aqueous AgPs suspension (25 mL) for 24 h. The stability analysis of the aqueous AgPs suspension was carried out as a variation of transmission (ΔT) and backscattering (ΔBS) profiles.

Electrodeposition of Zn/AgPs Composites Coatings

To evaluate the influence of surfactant concentration on the degree of occlusion of AgPs in the Zn/AgPs coatings, the CTAB surfactant concentration was varied during coating obtention.

Zn/AgPs composite coatings were formed for electrodeposition using a parallel plate cell with an interelectrode distance of 5 cm. A Zn plate (99%, Atotech) was used as the anode, and a plate of AISI 1018 steel with an exposed area of 10 × 15 cm^2 was used as the cathode. The temperature of the electrolytic bath was held at 25°C. The composition of the electrolytic bath was formulated and optimized in our laboratory (Meas et al., 2009; Trejo et al., 2002).

The electrodeposition current density (0.021 A cm^{-2} over 23 min) was selected on the basis of additional testing (not presented here) using a Hull cell. The electrodeposition of Zn/AgPs composite was carried out from a basic solution (S_0) + 2.5 mg L^{-1} AgNPs + x mM of CTAB, where x = 0.0, 0.05, 0.1, 0.5, 1.0, 10, or 50. All reagents were analytical grade, and the corresponding solutions were prepared with deionized water (18 MΩ cm^{-1} resistivity). In all cases, the pH of the working solution was 5.0. The morphology of each coating was evaluated using a scanning electron microscope (SEM) (Jeol Mod. JSM-6510LV) coupled to an energy dispersion spectrometer (EDS) analyzer (Bruker, Mod. Quantax 200), and the topography was analyzed using a profilometer (Veeco, Mod. Dektak 6M). The identification of the deposited phases was carried out by X-ray diffraction (XRD) using a Bruker diffractometer (Mod. D8 Advance, Bragg-Brentano arrangement) with Cu Kα-radiation (λ = 1.54°A). The 2θ range of 30 to 95° was recorded at a rate of 0.2° s^{-1}.

AFM Analysis

An atomic force microscope (AFM) (Digital Instruments, Mod. Nanoscope E, USA) and its own software was used in contact mode to image the deposited Zn/AgPs on the steel substrate. All AFM images of the samples were acquired at room temperature (25°C ± 1°C) and (44% ± 1%) relative humidity. These measurements were performed in air (ex situ) using silicon nitride AFM tips (Digital Instruments). The measurements were performed on scanning areas of 5 × 5 μm^2. The images were recorded at 2 Hz with a resolution of 512 × 512 pixels per image. The measurements were repeated for five times for each sample on

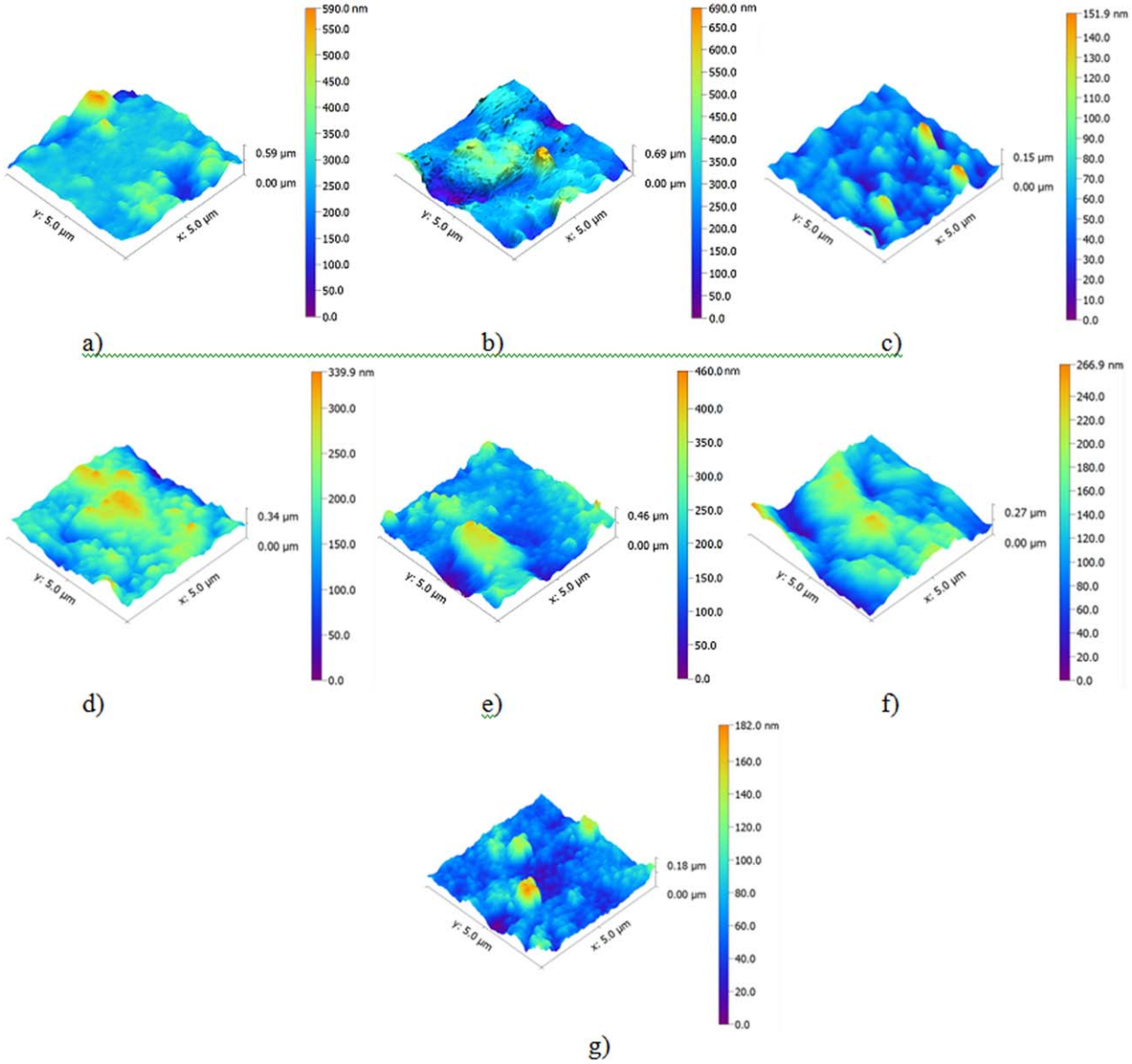

Fig. 1. The representative 3D topographic AFM images of the (Zn/AgPs) composite coatings surfaces: (**a**) ZnAgPm1 (0.0 mg cm^{-3} of Ag particles); (**b**) ZnAgPm2 (4.3 mg cm^{-3} of Ag particles); (**c**) ZnAgPm3 (5.6 mg cm^{-3} of Ag particles); (**d**) ZnAgPm4 (6.0 mg cm^{-3} of Ag particles); (**e**) ZnAgPm5 (6.4 mg cm^{-3} of Ag particles); (**f**) ZnAgPm6 (9.3 mg cm^{-3} of Ag particles); (**g**) ZnAgPm7 (14.1 mg cm^{-3} of Ag particles). Scanning square areas of 5 μm × 5 μm. The vertical range of the displayed data (in nanometers [nm]) and the colour bar are shown on the right side of the AFM image. [Color figure can be viewed in the online issue, which is available at wileyonlinelibrary.com.]

different reference areas to validate the reproducibility of the features.

Statistical Description of 3D Surface Roughness

Detailed information on the objective parameters used to obtain information on the basic properties of the height values distribution of the surface samples, according Gwyddion 2.37 software, is reported in the Appendix.

Statistical Analysis

Statistical analysis was performed using the SPSS 14 for Windows (Chicago, IL). One-way analysis of variance was used to test the differences between the two groups with Scheffé post-hoc tests for multiple comparisons. Differences with a P value of 0.05 or less were considered statistically significant. The average D_f results were expressed as mean value and standard deviation.

Fractal Analysis

Fractal analysis could offer new parameters for characterizing fractal patterns or sets of the morphology of a fractal object (Ţălu, 2012a). In this study, the fractal analysis was applied to the original AFM files using the cube counting method (derived directly from a definition of box-counting fractal dimension) with a

TABLE 1. The basic properties of the height values distribution (including its variance, skewness, and kurtosis) of the surface samples, for scanning square areas of 5 μm × 5 μm

The basic properties of the height values distribution of the surface samples	ZnAgPm1 samples	ZnAgPm2 samples	ZnAgPm3 samples	ZnAgPm4 samples	ZnAgPm5 samples	ZnAgPm6 samples	ZnAgPm7 samples
	Values	Values	Values	Values	Values	Values	Values
Maximum height (μm)	0.5892	0.6927	0.1519	0.3399	0.4558	0.2669	0.1820
Minimum height (μm)	0.0	0.0	0.0	0.0	0.0	0.0	0.0
Median height (μm)	0.2743	0.2656	0.0525	0.1880	0.1861	0.1285	0.0589
R_a (Sa) (μm)	0.0411	0.0727	0.0133	0.0386	0.0521	0.0342	0.0178
Rms (Sq) (μm)	0.0633	0.0949	0.0188	0.0496	0.0666	0.0418	0.0249
Skew (Ssk) (−)	0.63	0.35	1.31	0.0006	0.475	−0.0092	1.37
Kurtosis (Sku) (−)	3.78	0.722	4.09	0.213	0.338	−0.299	3.2
Inclination θ (°)	0.5	0.7	0.1	1.0	1.1	0.2	0.2
Inclination φ (°)	35.4	18.8	−5.4	−1.3	174.1	2.5	167.1

TABLE 2. The fractal dimensions (D) with coefficients of correlation (R^2) determined by the triangulation method, based on the linear interpolation type, of the (Zn/AgPs) composite coatings surfaces

Parameters	ZnAgPm1 samples	ZnAgPm2 samples	ZnAgPm3 samples	ZnAgPm4 samples	ZnAgPm5 samples	ZnAgPm6 samples	ZnAgPm7 samples
D	2.16 ± 0.005	2.19 ± 0.005	2.23 ± 0.005	2.18 ± 0.005	2.21 ± 0.005	2.14 ± 0.005	2.22 ± 0.005
R^2	0.992	0.993	0.994	0.991	0.993	0.992	0.991

linear interpolation type (the interpolated value in a point is calculated from the three vertices of the Delaunay triangulation triangle containing the point), which is described in detail in Gwyddion 2.37 software.

Wavelet Analysis of the 3D Surface Morphology

The wavelet transform (WT) is a useful tool of signal and image processing that have been successfully applied in the field of mechanical engineering to assess surface micro- and nano- topography (Adamczak et al., 2010; Stępień and Makieła, 2013).

To study the surface by the wavelet analysis, a two-dimensional discrete wavelet transform was conducted of the matrix containing values of heights of the surface. The wavelet transform was carried out in MATLAB with the use of Daubechies wavelet (the mother wavelet type was: db 5). In the study the single-level transform was performed (Adamczak et al., 2010; Stępień and Makieła, 2013).

RESULTS

The representative 3D topographic AFM images, for scanning square area of 5 × 5 μm^2, of the (Zn/AgPs) composite coatings surfaces is shown in Figure 1: (a) ZnAgPm1 (0.0 mg cm^{-3} of Ag particles); (b) ZnAgPm2 (4.3 mg cm^{-3} of Ag particles); (c) ZnAgPm3 (5.6 mg cm^{-3} of Ag particles); (d) ZnAgPm4 (6.0 mg cm^{-3} of Ag particles); (e) ZnAgPm5 (6.4 mg cm^{-3} of Ag particles); (f) ZnAgPm6 (9.3 mg cm^{-3} of Ag particles); (g) ZnAgPm7 (14.1 mg cm^{-3} of Ag particles). They are shown in 3D mode, in perspective view, with the vertical (height) scale (in nanometers [nm]) displayed in coding colors, according to the palette described by the respective side-bar on the right hand side of the AFM image.

The basic properties of the height values distribution of the surface samples (including its variance, skewness, and kurtosis), computed according Gwyddion 2.37 software is shown in Table 1.

A summary of the fractal dimensions with coefficients of correlation (R^2) determined by the triangulation method (computed according the Gwyddion 2.37 software), based on the linear interpolation type, of the (Zn/AgPs) composite coatings surfaces is shown in Table 2. The coefficients of correlation (R^2) of all linear fits were >0.990 representing a good linear correlation.

The wavelet analysis of the surfaces, for scanning square area of 5 × 5 μm^2, of the (Zn/AgPs) composite coatings samples associated with Figure 1, are shown in Figure 2. The colormap of the surfaces are shown in Figures 2a1–2g1 and the diagrams with values of the 1st level horizontal wavelet coefficients are presented in Figures 2a2–2g2.

The colormaps are shown in Figure 3 and they represent distributions of values of wavelet decomposition coefficients on analyzed surfaces. The areas where values of coefficients are changing significantly are marked with elypses.

DISCUSSION

Analyzing the AFM images of (Zn/AgPs) composite coatings fractal surfaces with statistical surface parameters, a specific 3D pattern of nanoasperities distribution is observed for different group of samples that occur at the micrometer- and nanometer-scale (Fig. 1).

The highest value of the maximum height is 0.6927 μm (second group), and the smallest value is 0.1519 μm (third group). The first group has the highest median height of 0.2743 μm, in contrast to the third group, wherein the median height is the lowest (0.0525 μm). The second group has the highest values of Sa (0.0727 μm) and Sq (0.0949 μm), whereas the lowest values belongs to the third group: Sa (0.0133 μm) and Sq (0.0188 μm). The biggest skewness (Ssk), qualifying the symmetry of the height distribution, is in the seventh group 1.37, and the smallest in the sixth group (−0.0092). The greatest value of the Kurtosis (Sku), qualifying the flatness of the height distribution, is for the third sample (4.09), and the smallest for the sixth one (−0.299). The inclination θ is the largest in the fifth group (1.1°), and the lowest in the third one (0.1°).

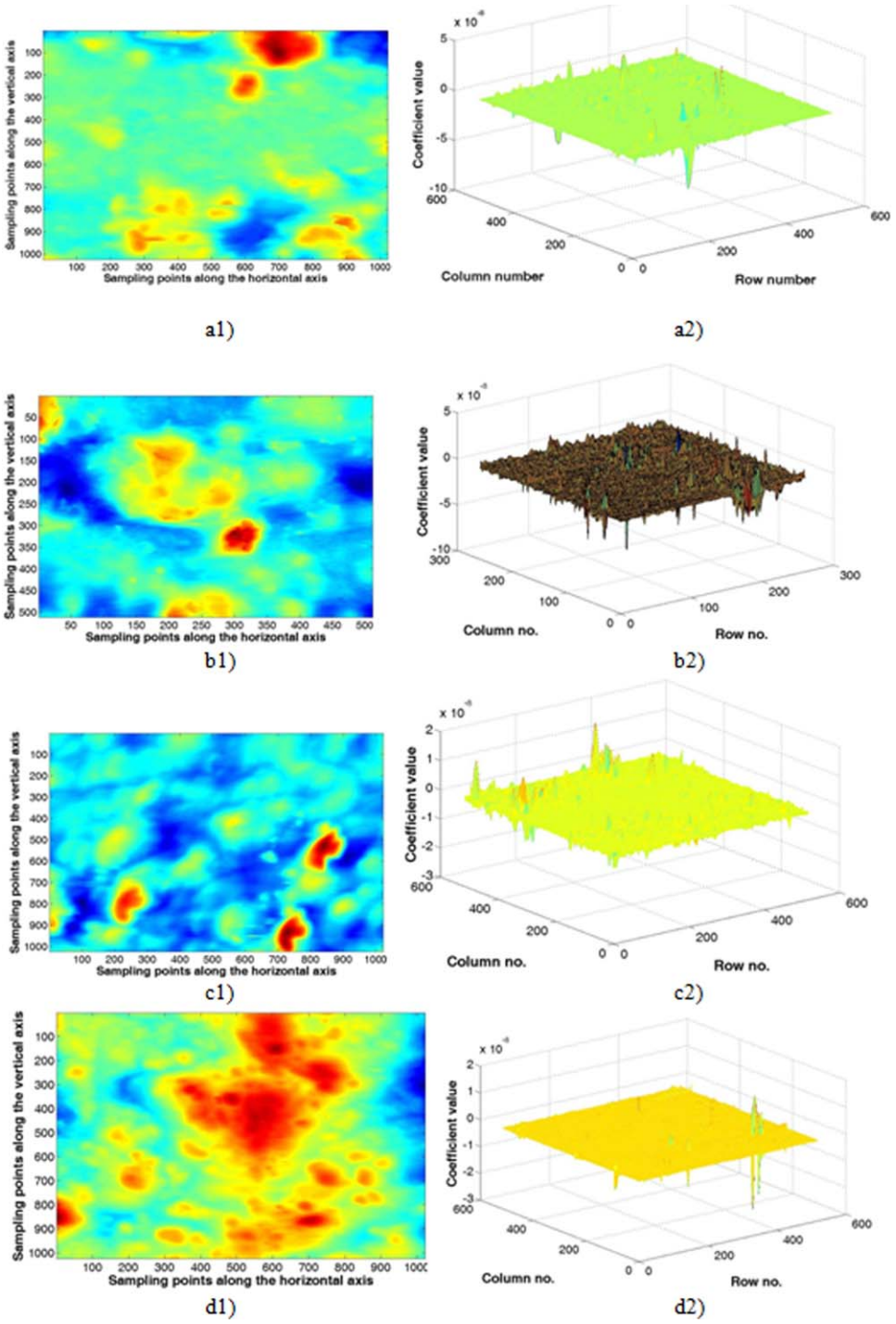

Fig. 2. Contour map of the (Zn/AgPs) composite coatings surfaces (index 1) and the wavelet horizontal details coefficients of the analyzed surface (index 2): (**a**) ZnAgPm1 (0.0 mg cm^{-3} of Ag particles); (**b**) ZnAgPm2 (4.3 mg cm^{-3} of Ag particles); (**c**) ZnAgPm3 (5.6 mg cm^{-3} of Ag particles); (**d**) ZnAgPm4 (6.0 mg cm^{-3} of Ag particles); (**e**) ZnAgPm5 (6.4 mg cm^{-3} of Ag particles); (**f**) ZnAgPm6 (9.3 mg cm^{-3} of Ag particles); (**g**) ZnAgPm7 (14.1 mg cm^{-3} of Ag particles). Scanning square areas of 5 μm × 5 μm. [Color figure can be viewed in the online issue, which is available at wileyonlinelibrary.com.]

The parameter inclination φ has the highest value, 174.1°, in the fifth group, and the smallest, equal to −5.4°, in the third group.

The higher fractal dimension D_f (average ± standard deviation) of 3D surfaces, as a measure of global scaling property, was found for the third group (2.23 ± 0.005), while the lower value was found for sixth group (2.14 ± 0.005). It can therefore be concluded that the smoothest surface is the third group, but the most regular one is the sixth group. A

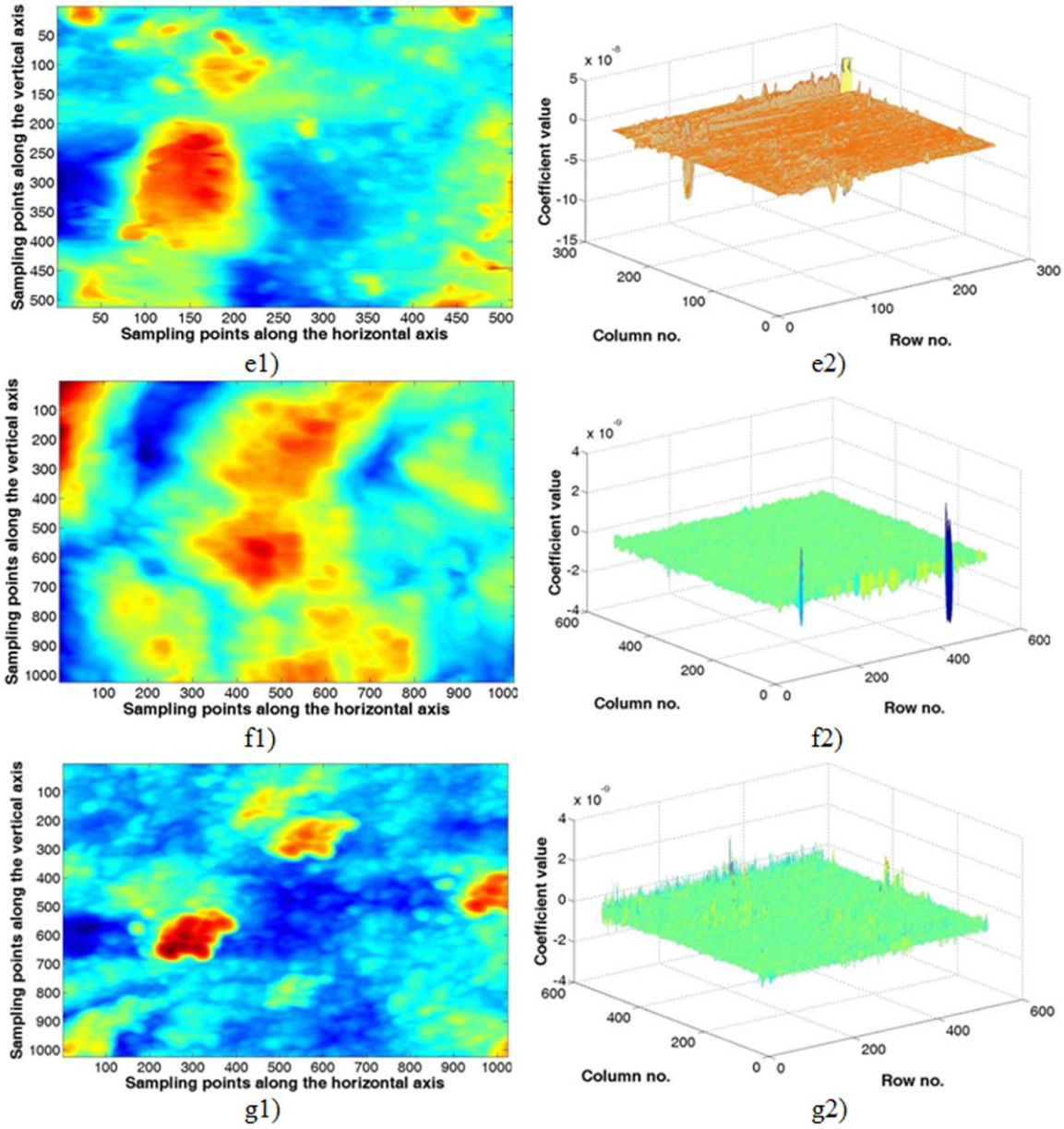

Fig. 2. (Continued). [Color figure can be viewed in the online issue, which is available at wileyonlinelibrary.com.]

significant correlation ($P < 0.05$) is observed and indicates that applied method is also correct in the analysis on samples 3D morphology.

The analysis of diagrams shown in Figure 2 reveals that all samples show a non-homogeneous surface with a specific 3D morphology that can be estimated by the wavelet transform. To analyze the difference between the values of wavelet decomposition coefficients for all analyzed surfaces, further study was conducted. The study involved more accurate analysis of changes of the values of wavelet decomposition coefficients. To do that a colormap of the values of the wavelet decomposition coefficients was generated for each analyzed surface.

The analysis of the diagrams shown in Figure 3 indicates that in most cases values of coefficients are quite similar on the whole analyzed surface.

In the case of diagrams shown in Figures 3a and 3g referring to samples ZnAgPm1 (0.0 mg cm^{-3} of Ag particles and ZnAgPm7 (14.1 mg cm^{-3} of Ag particles) there are more areas where values of wavelet decomposition coefficients change significantly. Nevertheless, one should note that coefficient values are relatively uniform besides the areas of sudden signal change.

The most uniform values of coefficients are in the case of the samples ZnAgPm6 (9.3 mg cm^{-3} of Ag particles) shown in Figure 3f and ZnAgPm4 (6.0 mg cm^{-3} of Ag particles) shown in Figure 3d. For these samples it is easy to notice that values of decomposition coefficients are similar to one another on the major parts of the surface and there are few areas where sudden change of the signal occurs.

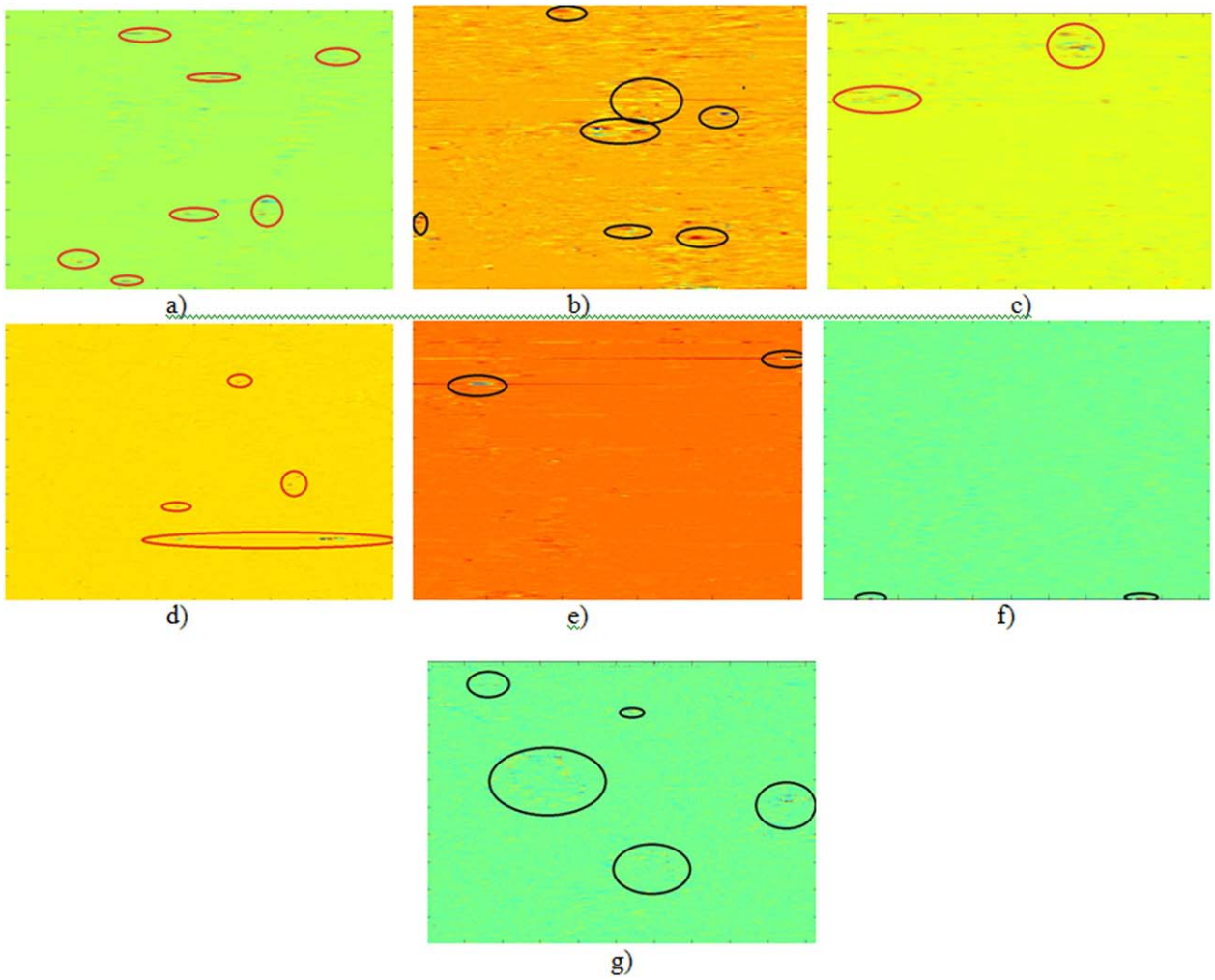

Fig. 3. Distribution of values of wavelet decomposition coefficients on the surface: (**a**) ZnAgPm1 (0.0 mg cm^{-3} of Ag particles); (**b**) ZnAgPm2 (4.3 mg cm^{-3} of Ag particles); (**c**) ZnAgPm3 (5.6 mg cm^{-3} of Ag particles); (**d**) ZnAgPm4 (6.0 mg cm^{-3} of Ag particles); (**e**) ZnAgPm5 (6.4 mg cm^{-3} of Ag particles); (**f**) ZnAgPm6 (9.3 mg cm^{-3} of Ag particles); (**g**) ZnAgPm7 (14.1 mg cm^{-3} of Ag particles). [Color figure can be viewed in the online issue, which is available at wileyonlinelibrary.com.]

Diagrams shown in Figures 3b, 3c, and 3e indicate that for the samples: ZnAgPm2 (4.3 mg cm^{-3} of Ag particles), ZnAgPm3 (5.6 mg cm^{-3} of Ag particles), and ZnAgPm5 (6.4 mg cm^{-3} of Ag particles) the differences between mutual values of wavelet decomposition coefficients are the highest ones. It is also easy to notice that these values are located isotropically (along the horizontal line).

CONCLUSION

Characteristic 3D topographic fractal parameter contributes substantially to evaluate the 3D surface micromorphology of (Zn/AgPs), which directly or indirectly influences the physical and the antibacterial effects properties and to provide a compact representation of complex morphologic information.

This study confirms the results obtained by Punith Kumar and Srivastava (2013), which demonstrated that the (Zn/AgPs) composite coatings surface morphology, depends on the material composition.

Our results suggest that AFM, the statistical surface roughness parameters, fractal analysis, and wavelet transform may provide additional insight in the surfaces engineering design and into the nature of the physical transformations that take place in the composite (Zn/AgPs) composite coatings. The height values distribution and fractal geometry-based parameters (fractal dimension D) have potential as tools for quantifying and identifying different 3D geometrical patterns in (Zn/AgPs) composite coatings, which could be extended to develop mathematical theoretical models which help to study structure, simulation of dynamics at interfaces, and thermodynamics processes at nanometer level.

APPENDIX

The basic properties of the height values distribution, including its variance, skewness, and kurtosis, computed according the Gwyddion 2.37 software and ISO 25178-2 is defined as follows:

- RMS value of the height irregularities: this quantity is computed from data variance.
- R_a value of the height irregularities: this quantity is similar to RMS value with the only difference in exponent (power) within the data variance sum. As for the RMS this exponent is $q = 2$, the R_a value is computed with exponent $q = 1$ and absolute values of the data (zero mean).
- Height distribution skewness: computed from 3rd central moment of data values. Negative skew indicates a predominance of valleys, while positive skew is seen on surfaces with peaks.
- Height distribution kurtosis: computed from 4th central moment of data values. For spiky surfaces, Sku > 3; for bumpy surfaces, Sku < 3; perfectly random surfaces have kurtosis of 3.
- Mean inclination of facets in area: computed by averaging normalized facet direction vectors.
- Variation, which is calculated as the integral of the absolute value of the local gradient.

REFERENCES

Adamczak S, Makieła W, Stępień K. 2010. Investigating advantages and disadvantages of the analysis of a geometrical surface structure with the use of Fourier and wavelet transform. Metrol Meas Syst 12:233–244.

Ahearn DG, May LL, Gabriel MM. 1995. Adherence of organisms to silver-coated surfaces. J Ind Microbiol 15:372–376.

Berezina S, Il'icheva AA, Podzorova LI, Ţălu Ş. 2015. Surface micromorphology of dental composites [CE-TZP]-[Al_2O_3] with Ca($^{+2}$) modifier. Microsc Res Tech 78:840–846. DOI: 10.1002/jemt.22548.

Chen HT, Ravishankar SA, Farinato RS. 2003. Rational polymer design for solid-liquid separations in mineral processing applications. Int J Miner Process 72:75–86.

Dallaeva D, Ţălu Ş, Stach S, Škarvada P, Tománek P, Grmela L. 2014. AFM imaging and fractal analysis of surface roughness of AlN epilayers on sapphire substrates. Appl Surf Sci 312:81–86. DOI: 10.1016/j.apsusc.2014.05.086.

Elenkova D, Zaharieva J, Getsova M, Manolov I, Milanova M, Stach S, Ţălu Ş. 2015. Morphology and optical properties of SiO_2-based composite thin films with immobilized Terbium(III) complex with a biscoumarin derivative. Int J Polym Anal Chem 20:42–56. DOI: 10.1080/1023666X.2014.955400.

Grier N. 1993. Silver and its compounds. In: Block SS, ed. Disinfection, sterilization and preservation. Philadelphia: Lea and Febiger. pp. 375–389.

Gwyddion 2.37 software (Copyright © 2004-2007, 2009-2014 Petr Klapetek, David Nečas, Christopher Anderson). Available at: http://gwyddion.net (last accessed July 31th, 2015).

ISO 25178-2, Geometrical product specifications (GPS)—Surface texture: Areal—Part 2: Terms, definitions and surface texture parameters. Available at: http://www.iso.org (last accessed July 31th, 2015).

Korai H. 1999. Current situation and future of inorganic antimicrobial agent. J Inorg Mater Jpn 6:428–436.

Kulesza S, Bramowicz M. 2014. A comparative study of correlation methods for determination of fractal parameters in surface characterization. Appl Surf Sci 293:196–201.

Lombardo M, Ţălu Ş, Ţălu M, Serrao S, Ducoli P. 2010. Surface roughness of intraocular lenses with different dioptric powers assessed by atomic force microscopy. J Cataract Refract Surg 36: 1573–1578. DOI: 10.1016/j.jcrs.2010.06.031.

Meas LEMY, Ortega-Borges R, Perez-Bueno JJ, Ruiz H, Trejo G. 2009. Effect of a poly (ethylene glycol)(MW 200)/benzylideneacetone additive mixture on Zn electrodeposition in an acid chloride bath. Int J Electrochem Sci 4:1735–1753.

Moldovan M, Prodan D, Popescu V, Prejmerean C, Saroşi C, Saplonţai M, Ţălu Ş, Vasile E. 2015. Structural and morphological properties of HA-ZnO powders prepared for biomaterials. Open Chem 13:725–733. DOI: 10.1515/chem-2015-0083.

Nguyen AV, Schulze HJ. 2004. Colloidal science of flotation. New York: Marcel Dekker.

Pabst W, Gregorova E. 2007. Characterization of particles and particle systems. Prague: ICT.

Punith Kumar MK, Srivastava C. 2013. Morphological and electrochemical characterization of electrodeposited Zn–Ag nanoparticle composite coatings. Mater Character 85:82–91. DOI: 10.1016/j.matchar.2013.08.017.

Reyes-Vidal Y, Suarez-Rojas R, Ruiz C, Torres J, Ţălu Ş, Méndez A, Trejo G. 2015. Electrodeposition, characterization, and antibacterial activity of zinc/silver particle composite coatings. Appl Surf Sci 342:34–41. DOI: 10.1016/j.apsusc.2015.03.037.

Stach S, Garczyk Ż, Ţălu Ş, Solaymani S, Ghaderi A, Moradian R, Nezafat Negin B, Elahi SM, Gholamali H. 2015. Stereometric parameters of the Cu/Fe NPs thin films. J Phys Chem C 119: 17887–17898. DOI: 10.1021/acs.jpcc.5b04676.

Senin N, Groppetti R. 2005. Surface microtopography design and manufacturing through topography descriptors: An application to prosthetic implant surfaces. Comp Aided Des 37:1163–1175. DOI: 10.1016/j.cad.2005.02.007.

Stępień K, Makieła W. 2013. An analysis of deviations of cylindrical surfaces with the use of wavelet transform. Metrol Meas Syst 20: 139–150.

Ţălu Ş. 1998. PhD. Thesis: Researches concerning the cold rolling process of external cylindrical threads, Technical University of Cluj-Napoca, Cluj-Napoca, Romania.

Ţălu Ş. 2012a. Mathematical methods used in monofractal and multifractal analysis for the processing of biological and medical data and images. Anim Biol Anim Husb 4:1–4.

Ţălu Ş. 2012b. Texture analysis methods for the characterisation of biological and medical images. Extreme Life Biospeol Astrobiol 4: 8–12.

Ţălu Ş. 2013. Characterization of surface roughness of unworn hydrogel contact lenses at a nanometric scale using methods of modern metrology. Polym Eng Sci 53:2141–2150.

Ţălu Ş, Stach S. 2014f. Multifractal characterization of unworn hydrogel contact lens surfaces. Polym Eng Sci 54:1066–1080. DOI: 10.1002/pen.23650.

Ţălu Ş, Stach S, Sueiras V, Ziebarth NM. 2014a. Fractal analysis of AFM images of the surface of Bowman's membrane of the human cornea. Ann Biomed Eng 43:906–916. DOI: 10.1007/s10439-014-1140-3.

Ţălu Ş, Stach S, Zaharieva J, Milanova M, Todorovsky D, Giovanzana S. 2014b. Surface roughness characterization of poly(methylmethacrylate) films with immobilized Eu(III) β-Diketonates by fractal analysis. Int J Polym Anal Chem 19:404–421. DOI:10.1080/1023666X.2014.904149.

Ţălu Ş, Stach S, Zaharieva J, Getsova M, Elenkova D, Milanova M. 2014c. Micromorphology characterization of SiO_2-based composite thin films with immobilized terbium(III) complex. Int J Polym Anal Chem 19:648–660. DOI: 10.1080/1023666X.2014.953749.

Ţălu Ş, Ghazai AJ, Stach S, Hassan A, Hassan Z, Ţălu M. 2014d. Characterization of surface roughness of Pt Schottky contacts on quaternary n-$Al_{0.08}In_{0.08}Ga_{0.84}N$ thin film assessed by atomic force microscopy and fractal analysis. J Mater Sci Mater Electron 25: 466–477. DOI: 10.1007/s10854-013-1611-6.

Ţălu Ş, Stach S, Méndez A, Trejo G, Ţălu M. 2014e. Multifractal characterization of nanostructure surfaces of electrodeposited Ni-P coatings. J Electrochem Soc 161:D44–D47.

Ţălu Ş, Stach S, Lainović T, Vilotić M, Blažić L, Alb SF, Kakaš D. 2015a. Surface roughness and morphology of dental nanocomposites polished by four different procedures evaluated by a multifractal approach. Appl Surf Sci 330:20–29. DOI: 10.1016/j.apsusc.2014.12.120.

Ţălu Ş, Stach S, Valedbagi S, Elahi SM, Bavadi R. 2015b. Surface morphology of titanium nitride thin films synthesised by DC reactive magnetron sputtering. Mater Sci Poland 33:137–143. DOI: 10.1515/msp-2015-0010.

Ţălu Ş, Stach S, Ghodselahi T, Ghaderi A, Solaymani S, Boochani A, Garczyk Ż. 2015c. Topographic characterization of Cu–Ni NPs @ a-C:H films by AFM and multifractal analysis. J Phys Chem B 119: 5662–5670.

Ţălu Ş, Stach S, Solaymani S, Moradian R, Ghaderi A, Hantehzadeh MR, Elahi SM, Garczyk Ż, Izadyar S. 2015d. Multifractal spectra of atomic force microscope images of Cu/Fe nanoparticles based films thickness. J Electroanal Chem 749:31–41. DOI: 10.1016/j.jelechem.2015.04.009.

Trejo G, Ortega R, Meas Y. 2002. The effect of the PEG 8000 additive on the deposition mechanism and morphology of zinc deposits. Plating Surf Finish 89:84–87.

Zhang XG. 1996. Corrosion and electrochemistry of zinc. New York: Plenum Press.